DOI: 10.1109/IPIN.2019.8911743

Experimental Evaluation of Round-Trip ToF-based Localization in the 60 GHz Band

Nebojsa Maletic*, Vladica Sark*, Marcus Ehrig*, Jesús Gutiérrez* and Eckhard Grass*†
*IHP – Leibniz-Institut für innovative Mikroelektronik
15236 Frankfurt (Oder), Germany
†Humboldt-Universität zu Berlin
12489 Berlin, Germany
Email: {maletic; sark; ehrig; teran; grass}@ihp-microelectronics.com

***Abstract*—Millimeter wave (mmWave) communication has emerged as a key technology for achieving high data throughput and low latency in 5G networks. Thanks to the large channel bandwidths in the mmWave spectrum (e.g. 2.16 GHz in the 57-66 GHz band), mmWave technology allows precise and accurate time of flight (ToF) measurements, hence supporting precise and accurate positioning. In this paper, an experimental evaluation of ToF-based localization in the 60 GHz band is presented. We implemented the two-way ranging (TWR) protocol between a mobile node and multiple anchor nodes. The implementation is carried out on an own software-defined radio (SDR) baseband platform, combined with commercial 60 GHz chipsets. Tests were performed indoors in a laboratory environment. The results of our evaluation show that a positioning error of less than 5 cm can be obtained.**

***Index Terms*—Localization, time of flight (ToF), two-way ranging (TWR), millimeter wave, software-defined radio (SDR), 60 GHz**

I. Introduction

The fifth generation (5G) of mobile communication networks are anticipated to provide a massive leap when compared to the existing networks in terms of system capacity, data throughputs, end-to-end latency, seamless coverage (via dense small cells), number of connected devices, network energy efficiency, etc. [1], [2]. Besides, highly accurate device positioning and location-aware communication are envisioned. The positioning accuracy is expected to be in the order of a meter or even sub-meter [3], [4]. Such a high-performance positioning is essential for new emerging applications and location-based services, including safety-critical applications, augmented reality [5], assisted living [6], healthcare and emergency services [4], etc. In addition, positioning information can be used as support for channel estimation or to perform beamforming by steering transmission towards a user (with known position), therefore reducing the beam search time.

To address the challenges of 5G, several technologies have emerged, among which, millimeter wave (mmWave) is regarded as the key one for achieving high data rates and low latency communication [7], [8]. Apart from the communications viewpoint, mmWave technology offers a significant improvement in positioning accuracy. Given the large signal bandwidths, good separation of multipath components is possible as well as highly accurate time of arrival (ToA) estimation.

To this end, mmWave-based localization has attracted considerable attention in the research community. In [9], [10], conventional localization methods using different signal parameters such as received signal strength (RSS), ToA and time difference of arrival (TDoA) were investigated. A mmWave localization and tracking method using RSS and signal phase, called mTrack, is proposed in [11]. In [12], a mmWave localization method, which is environment blind, is proposed. Simultaneous localization and mapping (SLAM) using mmWaves has been investigated in [13]. Different methods for localization using a single anchor node exploiting multi-reflected paths are given in [14]. A joint localization and position orientation system using mmWave is investigated in [15]. In [16] authors analyzed the impact of beamforming strategies on mmWave localization. The use of both Sub-6 GHz band and mmWave for localization purposes is investigated in [17], with the Sub-6 GHz band being suitable for angle of arrival (AoA) estimation, and the mmWave band for precise distance estimation. Combining the two, the position information can be easily obtained. In [18], angle information is leveraged from the sector scanning carried out by the firmware of mmWave devices for beam training and link establishment. A sub-meter accuracy is achieved in most of the cases, even in the presence of only a single access node.

This paper deals with device localization in the 60 GHz ISM band under a line-of-sight (LoS) scenario. In fact, this work is a follow-up of our work in [19], in which a wavelength precise and accurate distance estimation (i.e. ranging) using two-way ranging over 1 GHz wide channel in the 60 GHz band was achieved. Here, we take a step further and perform round-trip ToF (RTToF) localization. We implement the TWR protocol with multiple anchor nodes on a custom high-performance system-on-chip (SoC) baseband platform. The experimental results, performed in an indoor environment, show a positioning error of less than 5 cm.

The rest of this paper is organized as follows: a brief discussion on lateration-based positioning and the TWR method is given in Section II. The same section provides details on our approach of implementing 60 GHz RTToF localization. Our

The research leading to these results has received funding from the European UnionâĂŹs Horizon 2020 research and innovation programme, WORTECS project, under grant agreement No 761329; its content reflects the view of its authors only.

localization testbed and measurement setup with the results and the accompanying discussion are covered in Section III. Section IV concludes the paper and suggests topics for future work.

II. RTTOF Localization Method

A. Lateration: Background

The basic localization scenario includes a few anchor nodes (3 or more for 2D localization), with reference (known) positions, as well as mobile nodes, whose positions are to be estimated. To achieve high accuracy and precision while maintaining low system complexity, localization algorithms based on RTToF ranging (distance estimates) are preferred.

The process of finding the location of a mobile device based on the distances between a mobile and the anchor nodes is called *circular lateration*. When the number of anchor nodes is n = 3, the process is termed *trilateration*. Fig. 1 depicts this situation. The position of the mobile node is obtained as a result of the intersection of the three circles. The distances measured from each of the anchor nodes to the mobile node are the radii of the circles. Mathematically, the distance between an unknown mobile node with coordinates (x, y), and n anchor nodes with known coordinates (X_i, Y_i) is given by

$$r_i = \sqrt{(X_i - x)^2 + (Y_i - y)^2}, i = 1, ..., n. \tag{1}$$

A system of n nonlinear equations can be formed, where (x, y) is the unknown position and r_i are the measured distances. The solution is found using, for example the least-squares approach or iterative methods. The distances between the anchor points and the mobile device r_i are typically obtained via ToF measurements.

Two main approaches are used for distance estimation, namely ToA and RTToF, where the latter is commonly referred to as TWR or two-way ToF (TW-ToF). The ToA method requires precise synchronization of all nodes (in order of sub-nanoseconds), which cannot be easily achieved. Therefore, TWR is the preferred method, as it significantly reduces synchronization requirements as compared to the former.

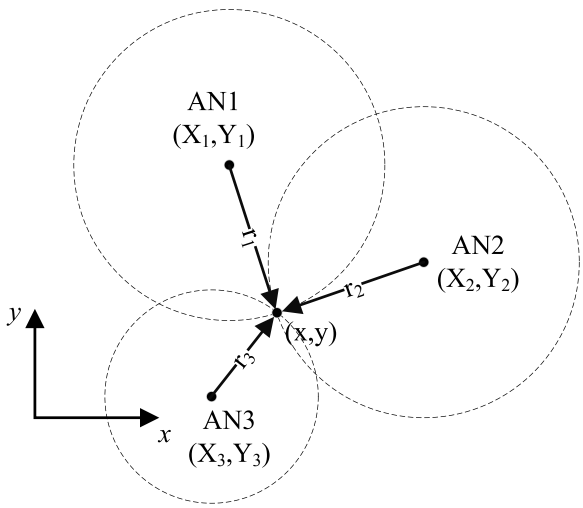

Fig. 1. Illustration of the trilateration algorithm.

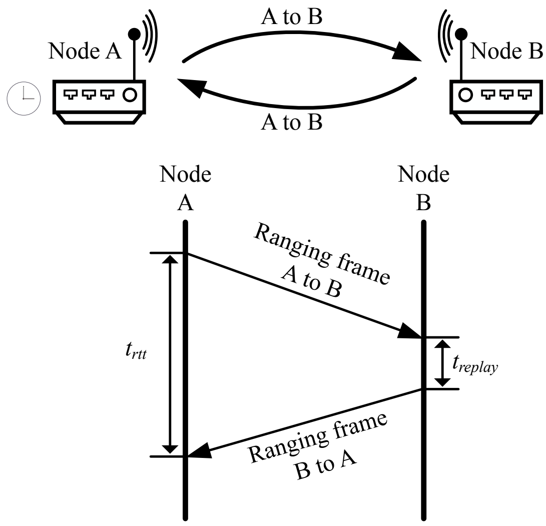

Fig. 2. Two-way ranging protocol.

B. The Two-way Ranging Method

In a TWR scenario, a known signal - usually a frame with a known pseudo-noise (PN) sequence - is sent from node A to node B (see Fig. 2). Node B replies to node A after a replay time, t_{replay}. Node A measures how much time it takes for the signal to travel from A to B and back to A. Knowing the reply time of node B, the time of flight, t_{tof}, and, therefore, the distance, r, can be calculated as follows

$$t_{tof} = \frac{t_{rtt} - t_{replay}}{2}, \quad r = c \cdot t_{tof}. \tag{2}$$

Here, t_{rtt} is the round-trip time and $c \simeq 3e8$ m/s is the speed of light. Only a coarse synchronization is needed in this case, which is required for reserving a time slot for the TWR process. The precision of this synchronization is usually larger than one microsecond, which is possible with present-day wireless communication systems.

By performing TWR between a mobile node and each anchor node, the corresponding distances, r_i, from (1) can be obtained.

C. Implementation

In this section, we present the implementation of the localization algorithm based on a TWR protocol with multiple anchor nodes working in the 60 GHz band. This work is a continuation of the work given in [19]. In our localization scenario, a configuration having a single master and multiple slave nodes is chosen. The role of the master is assigned to a mobile device, while the anchors are slave nodes. Typically, scheduling of localization (hence, ranging) slots is made by a point-to-multiple-point (P2MP) Medium Access Control (MAC) processor. Nevertheless, to ease implementation for our experiments, an SDR approach is favored. This means, most of the ranging processing is carried out in software. Therefore,

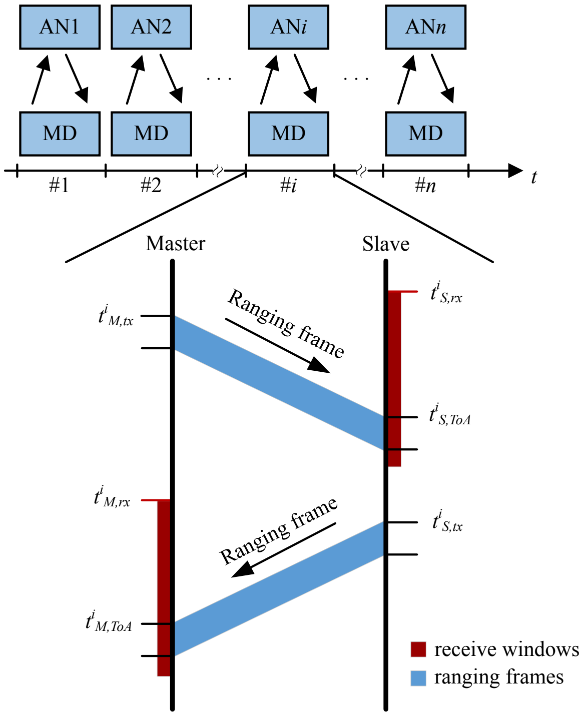

Fig. 3. Implementation of the RTToF-based localization.

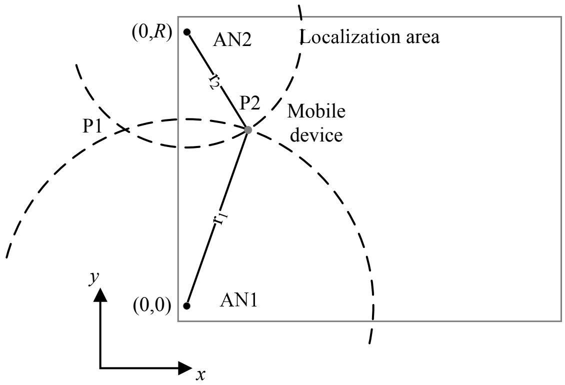

Fig. 4. Localization testbed.

in our experimental SDR approach, there is no MAC processor and the scheduling of ranging slots is performed by the master node over a dedicated trigger cable. This does not affect the generality or quality of the obtained results.

Fig. 3 describes the main implementation idea. The time is divided into time slots, wherein each time slot a TWR is performed between the master (i.e. mobile device, MD) and corresponding slave node (i.e. anchor, AN). We use the two-way ranging method based on receive windows, already described in [19], [20]. In this method, ranging frames are expected to arrive during receive window periods scheduled in advance. Thus, the receive windows should be synchronized with the transmissions. In the absence of a MAC processor scheduling the ranging process, we use dedicated synchronization (or trigger) via a cable.

The procedure work as follows. Ranging frames are prepared in Matlab and stored in the memory of the master node and all slave nodes. Further, a send command is issued to the master node and the transmit timestamp, $t^i_{M,tx}$, is retrieved. At the same time, a receive window start is triggered at the i-th slave node over the dedicated synchronization cable. The start of the receive window is timestamped with a timestamp $t^i_{S,rx}$. Within the receive window, the received samples are stored in the memory of the slave node. Upon termination of the receive window, a frame, previously stored in the memory of the i-th slave node, is transmitted at a time, $t^i_{S,tx}$, to the master node and the receive window at the master node is triggered via cable at time $t^i_{M,rx}$. The samples within the receive window are stored in the memory. All transmit and receive window times are timestamped and recorded. At this point, the received samples at both nodes are processed in Matlab for ToA estimation. By performing cross-correlation of the received samples with a locally stored ranging sequence, ToA at the i-th slave node, $t^i_{S,ToA}$ and ToA at the master node, $t^i_{M,ToA}$ are estimated. Finally, the distance is estimated according to

$$r_i = \frac{c}{2}\big(t^i_{M,rx} - t^i_{M,tx} + t^i_{M,ToA} + t^i_{S,rx} - t^i_{S,tx} + t^i_{S,ToA}\big). \quad (3)$$

The above procedure is repeated with all slave (i.e. anchor) nodes.

III. Experiment and Results

In this section, we present the measurement results of the implementation of RTToF localization in the 60 GHz band. At first, the localization testbed and the used hardware are described. Afterward, results of the measurements are given and discussed.

A. Testbed and Measurement Setup

The localization testbed is shown in Fig. 4. By placing the anchor nodes in the corners of the area in which the mobile device needs to be localized, it is possible to exclude some potential positioning results (e.g. point P1), which are implausible given the defined geometry of the localization area. This reduces the number of necessary anchor nodes to two, for a 2D localization. Hence, knowing the exact location of anchor nodes (AN1 and AN2), the position of the mobile device can be determined by applying simple trigonometry.

Let (x_{AN1}, y_{AN1}) = (0, 0) and (x_{AN2}, y_{AN2}) = (0, R) be the coordinates of anchor nodes AN1 and AN2, respectively, with R denoting the distance between them. The position of the mobile device (x_m, y_m) can be obtained as follows

$$r_1^2 = x_m^2 + y_m^2, \quad r_2^2 = x_m^2 + (y_m - R)^2, \quad (4)$$

$$x_m = \sqrt{r_1^2 - y_m^2}, \quad y_m = \frac{r_1^2 - r_2^2 + R^2}{2R}. \quad (5)$$

In the above equations, r_1 and r_2 are the distances between the mobile node and the two anchor nodes. The distance, R, between the two anchor nodes is known, while r_1 and r_2

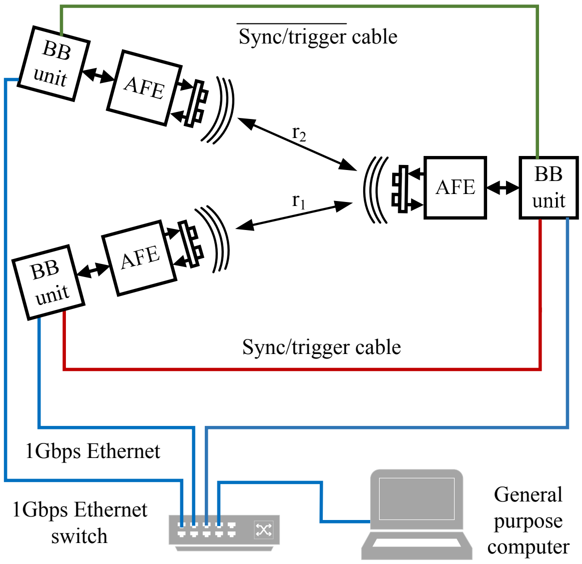

Fig. 5. Measurement setup.

are estimated from the TWR measurements, as explained in Section II-C.

The measurement setup, an illustration is shown in Fig. 5, consists of three nodes, two being fixed (ANs) and the third mobile. All nodes are equipped with a baseband (BB) unit and a commercial mmWave analog front-end (AFE). The BB unit is a universal SoC FPGA platform intended for mmWave applications [21]. It can be used as an SDR or a real-time platform, and it features a high-performance FPGA-ARM-SoC Zynq-7045, 2.16 GSps data converters and Gigabit Ethernet transceivers. The used AFEs are the 60 GHz evaluation boards with transmitter and receiver chips and integrated antennas from Hittite [22]. The cosine-squared beam-shaped antenna has 7.5 dBi gain and 60° half-power beamwidth. Three nodes are connected to a PC through an Ethernet switch. The PC controls signal transmission and reception with processing performed in Matlab. An image of the system setup in a laboratory with the used hardware is depicted in Fig. 6.

For the ranging (i.e. distance estimation), an *m*-sequence of 1023 chips length is used. The sequence is BPSK modulated and filtered using a square-root raised cosine (SRRC) filter with a roll-off factor of one and oversampling factor of 2, yielding the 3-dB modulation bandwidth of around 1 GHz. The experiment was carried out in a laboratory. Measurements were performed at 8 randomly chosen positions at the carrier frequency of 60 GHz. At each location, 100 ranging measurements per anchor node are recorded. To each AN, the reference distance is measured with a professional laser distance meter. The distance between two anchor nodes was R = 1.8 m and the setupâĂŹs height was 73.5 cm. Due to the short length of the trigger cable, the localization area is bounded to the size of 1.8×2 m^2.

B. Localization Results

Fig. 7 depicts the obtained 2D positioning map of the mobile device, where both true locations and the estimated positions (100 estimates per location), relative to the locations of ANs, are shown. A relatively small spread of the estimated positions around the true ones is observed.

The precision of the ranging estimation is analyzed by means of the cumulative distribution function (CDF) of the distance errors for each AN. The derived CDF of the ranging estimates is shown in Fig. 8, for AN1 left and AN2 right. In both cases, the absolute ranging error is below 30 mm. Moreover, the absolute ranging error is around 15 mm (3× the wavelength at 60 GHz) in 80% of the obtained results. In [19], we achieved the absolute ranging error of 9 mm. Compared to this work, in [19] high gain antennas were used, and Tx and Rx beams were aligned as well to have a high signal-to-noise ratio (SNR) for signal reception. We posit that, by having a 60 GHz system with beam-steering/-tracking capability, the ranging performance as reported in [19] can be achieved, since beam alignment can be maintained by a beam tracking mechanism.

The positioning error is calculated as the Euclidean distance between the estimated ($\hat{x}$, $\hat{y}$) and true position (x, y)

$$\lambda_k^l = \sqrt{(\hat{x}_k^l - x_k^l)^2 + (\hat{y}_k^l - y_k^l)^2},$$
$$l = 1, ..., 8, k = 1, ..., 100. \tag{6}$$

For each location l, $\Lambda_l = \{\lambda_1^l, ..., \lambda_{100}^l\}$ represents the set of positioning errors, such that mean, maximal and minimal positioning errors are obtained as $\overline{\Lambda}_l$, $max(\Lambda_l)$ and $min(\Lambda_l)$, respectively, where $\overline{(\cdot)}$ denotes the mean. This is summarized in Fig. 9. The lowest mean error was 6.8 mm and the largest was 12.4 mm. The average positioning error across all locations equals 8.828 mm with a standard deviation of 5.63 mm.

The CDF of the positioning error for each location is shown in Fig. 10. The positioning error remains below 5 cm. From Fig. 7 and Fig. 9 it can be observed that the largest errors occur at the location 8. This is due to the geometrical setup and could be improved with an additional anchor node in the right (east) region of the experimental area. In [19], it was shown that the ranging error is Gaussian distributed. Therefore, it is interesting to analyze the distribution of the positioning error, $f_\lambda(\lambda)$. Following the approach in [19], the Kolmogorov-Smirnov (K-S) test [23] is used to find the best-fitted distribution. The idea is to verify whether the data comes from a specific, continuous distribution, by measuring the distance between the empirical CDF and the CDF of the reference distribution. The histogram of the positioning error (integrated over all locations) with the fitted reference distribution is depicted in Fig. 11.

It can be noted that the positioning error follows quite well Gamma distribution [24] with the shape parameter α = 2.593, and the scale parameter β = 0.3405, i.e. $f_\lambda(\lambda)$ = $Gamma(\alpha, \beta)$. The corresponding CDF, shown in Fig. 10, is given by $F_\lambda(\lambda) = \gamma(\alpha, \lambda/\beta)/\Gamma(\alpha)$, where $\gamma(\cdot, \cdot)$ is the lower

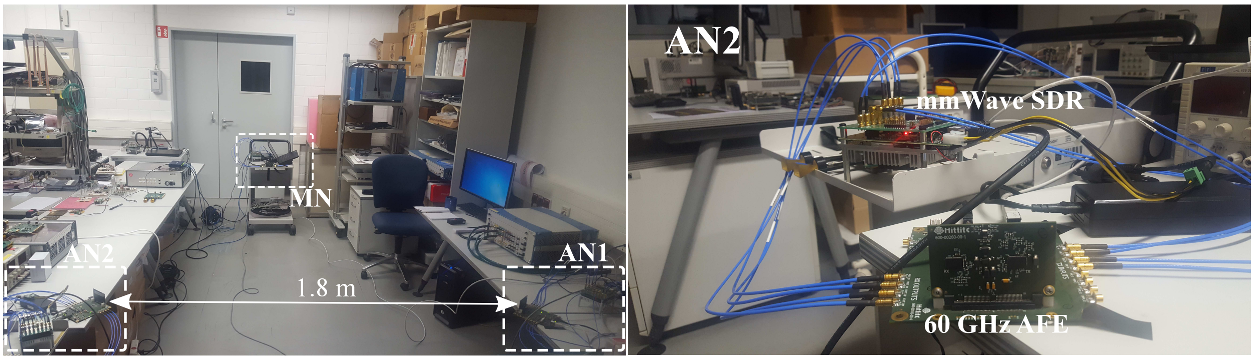

Fig. 6. An image of the system setup in a laboratory (left) and the used hardware (right).

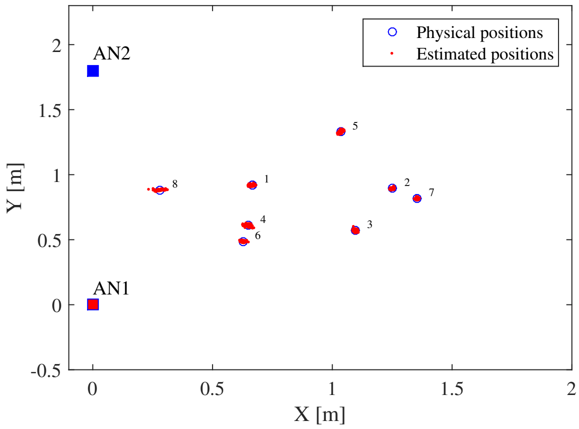

Fig. 7. Estimated vs. physical positions.

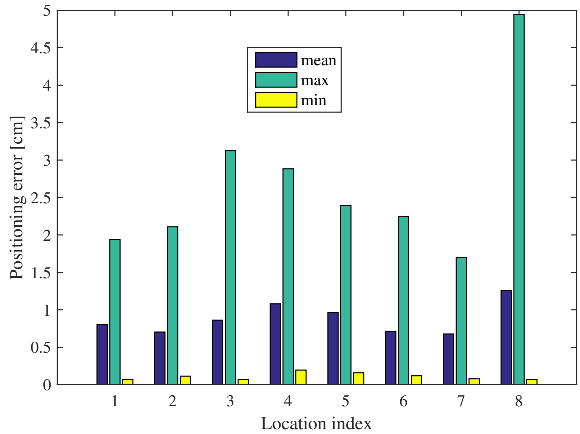

Fig. 9. Mean, max and min positioning error per location.

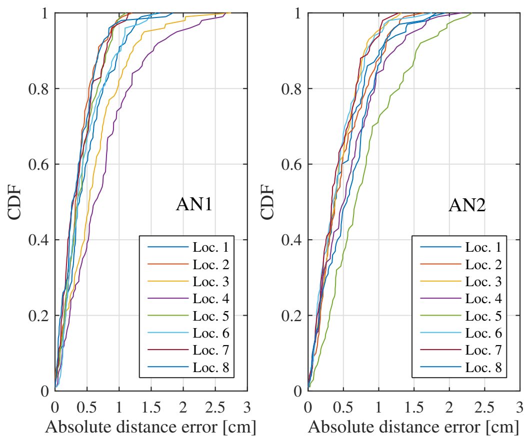

Fig. 8. CDF of the ranging error (AN1-left, AN2-right).

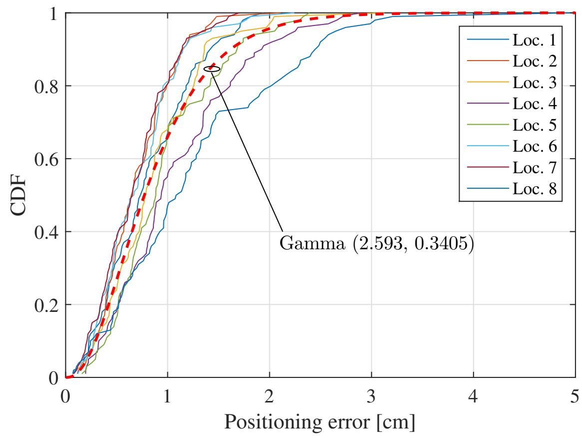

Fig. 10. CDF of the positioning error.

incomplete Gamma function [25] and $\Gamma(s) = (s-1)!$. Based on the properties of the Gamma distribution, we can analytically obtain mean and standard deviation of the positioning error as

$$\mathtt{E}(\lambda) = \alpha \cdot \beta = 0.8829 \text{ cm}, \quad (7)$$

$$\mathtt{Std}(\lambda) = \sqrt{\alpha} \cdot \beta = 0.5483 \text{ cm}. \quad (8)$$

The calculated mean and standard deviation match well the values obtained from measurements. Nevertheless, to get more insights into the nature of parameters of the fitted distribution, it would be welcomed to derive the distribution of the positioning error analytically w.r.t. ranging errors for the underlying localization scenario. This kind of analysis is left for future work.

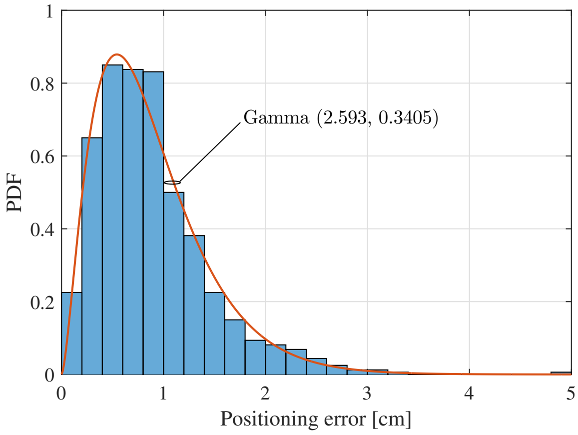

Fig. 11. Distribution of the positioning error.

IV. Conclusion and Future Work

In this work, time of flight (ToF) based localization in the 60 GHz band has been presented and evaluated. A two-way ranging (TWR) protocol with multiple anchors has been implemented on a custom millimeter wave (mmWave) software-defined radio (SDR) baseband platform following an SDR approach to ease the implementation effort. The implemented algorithm has been tested indoors in a laboratory environment.

The results of the distance estimates have shown that the absolute ranging error per anchor node is below 3 cm, whereas the achieved positioning error is below 5 cm. Although the algorithm was tested in a static scenario, this exceptional result demonstrates that mmWave technology is extremely well suited to achieve sub-meter positioning accuracy, as required in 5G networks.

For future work, there are several directions to be pursued. To improve ranging estimates and, thereby, reduce positioning error, beamforming analog front-end (AFE) modules coupled with beam tracking should be used. With proper beam alignment, signal-to-noise ratio (SNR) can be kept at a high level, enabling precise ToF measurements. This way, a few millimeters of ranging accuracy, as reported in [19], can be achieved. Performing measurements with three or more anchors will improve the positioning performance and make the localization system more robust. Furthermore, evaluation should be extended to harsh environments to positioning and include mobility scenario. In the latter, localization can be coupled with some tracking mechanism (e.g. extended Kalman filter or particle filter) and/or a user motion dynamics. Finally, single mmWave anchor positioning combining ranging with angulation is one more direction to follow.

References

[1] J. G. Andrews et al., "What Will 5G Be?," IEEE J. Sel. Areas Commun., vol. 32, no. 6, 2014, pp. 1065-1082

[2] M. Shafi et al., "5G: A Tutorial Overview of Standards, Trials, Challenges, Deployment, and Practice," IEEE J. Sel. Areas Commun., vol. 35, no. 6, 2017, pp. 1201-1221.

[3] M. Koivisto et al., "High-Efficiency Device Positioning and Location-Aware Communications in Dense 5G Networks," IEEE Commun. Mag., vol. 55, no. 8, 2017, pp. 188-195

[4] Y. Liu, X. Shi, S. He and Z. Shi, "Prospective Positioning Architecture and Technologies in 5G Networks," IEEE Netw., vol. 31, no. 6, 2017, pp. 115-121

[5] M. Ehrig et al., "Reliable Wireless Communication and Positioning Enabling Mobile Control and Safety Applications in Industrial Environments," IEEE International Conference on Industrial Technology (ICIT), Toronto, 2017, pp. 1301-1306

[6] K. Witrisal et al., "High-Accuracy Localization for Assisted Living: 5G Systems Will Turn Multipath Channels From Foe to Friend," IEEE Sig. Proces. Mag., vol. 33, no. 2, 2016, pp. 59-70

[7] W. Roh et al., "Millimeter-Wave Beamforming as an Enabling Technology for 5G Cellular Communications: Theoretical Feasibility and Prototype Results," IEEE Commun. Mag., vol. 52, no. 2, 2014, pp. 106-113

[8] T. S. Rappaport et al., "Millimeter Wave Mobile Communications for 5G Cellular: It Will Work!", IEEE Access, vol. 1, 2013, pp. 335-349

[9] H. El-Sayed, G. Athanasiou and C. Fischione, "Evaluation of Localization Methods in Millimeter-Wave Wireless Systems," IEEE 19th International Workshop on Computer Aided Modeling and Design of Communication Links and Networks (CAMAD), Athens, pp. 345-349, 2014

[10] F. Lemic et al., "Localization as a Feature of mmWave Communication," International Wireless Communications and Mobile Computing Conference (IWCMC), Paphos, pp. 1033-1038, 2016

[11] T. Wei et al., "mTrack: High-Precision Passive Tracking using Millimeter Wave Radios," in Mobile Computing and Networking, ACM, pp. 117-129, 2015

[12] J. Palacios, P. Casari and J. Widmer, "JADE: Zero-knowledge Device Localization and Environment Mapping for Millimeter Wave Systems," IEEE INFOCOM 2017-IEEE Conference on Computer Communications, Atlanta, GA, 2017, pp. 1-9.

[13] F. Guidi, A. Guerra and D. Dardari, "Millimeter-Wave Massive Arrays for Indoor SLAM," 2014 IEEE International Conference on Communications Workshops (ICC), Sydney, pp. 114-120, 2014

[14] A. Olivier et al., "Lightweight Indoor Localization for 60-GHz Millimeter Wave Systems," IEEE International Conference on Sensing, Communication and Networking (SECON), pp. 27-30, London, 2016

[15] A. Shahmansoori, G. E. Garcia, G. Destino, G. Seco-Granados and H. Wymeersch, "5G Position and Orientation Estimation through Millimeter Wave MIMO," 2015 IEEE Globecom Workshops (GC Wkshps), San Diego, CA, 2015, pp. 1-6. doi: 10.1109/GLOCOMW.2015.7413967

[16] A. Guerra, F. Guidi and D. Dardari, "On the Impact of Beamforming Strategy on mm-Wave Localization Performance Limits," IEEE ICC Workshop on Advances in Network Localization and Navigation (ANLN), Paris, pp. 809-814, 2017

[17] N. Maletic, V. Sark, J. GutiÃĺrrez and E. Grass, "Device Localization Using mmWave Ranging with Sub-6-Assisted Angle of Arrival Estimation," 2018 IEEE International Symposium on Broadband Multimedia Systems and Broadcasting (BMSB), Valencia, 2018, pp. 1-6.

[18] J. Palacios et al, "Single- and Multiple-Access Point Indoor Localization for Millimeter-Wave Networks," Trans. on Wireless Commun., vol. 18. no. 3, 2019, pp. 1927-1942

[19] V. Sark, N. Maletic, M. Ehrig, J. GutiÃĺrrez and E. Grass, "Achieving Millimeter Precision Distance Estimation using Two-way ranging in the 60 GHz Band," proc. of the 28th European Conference on Networks and Communications (EuCNC), in Valencia, in press.

[20] V. Sark, N. Maletic, J. GutiÃĺrrez and E. Grass, "An Approach for Implementation of Ranging and Positioning Methods on a Software Defined Radio," 14th Workshop on Positioning, Navigation and Communications (WPNC), Bremen, 2017, pp. 1-6.

[21] M. Petri and M. Ehrig, "A SoC-based SDR Platform for Ultra-High Data Rate Broadband Communication, Radar and Localization Systems," 2019 Wireless Days (WD), Manchester, United Kingdom, 2019, pp. 1-4. doi: 10.1109/WD.2019.8734240

[22] https://www.analog.com/en/products/hmc6000.html Accessed April 25, 2019.

[23] Chakravarti, Laha, and Roy, *Handbook of Methods of Applied Statistics*, Volume I, John Wiley and Sons, 1967, pp. 392-399

[24] Weisstein, Eric W. "Gamma Distribution." From MathWorld–A Wolfram Web Resource. http://mathworld.wolfram.com/ GammaDistribution.html, Accessed April 25, 2019.

[25] Abramowitz, M. and Stegun, I. A. (Eds.). *Handbook of Mathematical Functions with Formulas, Graphs, and Mathematical Tables*, 9th printing. New York: Dover, p. 260, 1972.